

Effect of nearest neighbor repulsion on the low frequency phase diagram of a quarter-filled Hubbard-Holstein chain

Philippe Maurel and Marie-Bernadette Lepetit*
*Laboratoire de Physique Quantique & UMR 5626 du CNRS,
Université Paul Sabatier, F-31062 Toulouse Cedex 4, France*

(Dated: October 30, 2018)

We have studied the influence of nearest-neighbor (NN) repulsions on the low frequency phases diagram of a quarter-filled Hubbard-Holstein chain. The NN repulsion term induces the apparition of two new long range ordered phases (one $4k_F$ CDW for positive $U_{eff} = U - 2g^2/\omega$ and one $2k_F$ CDW for negative U_{eff}) that did not exist in the $V = 0$ phases diagram. These results are put into perspective with the newly observed charge ordered phases in organic conductors and an interpretation of their origin in terms of electron molecular-vibration coupling is suggested.

I. INTRODUCTION

It is well known that low dimensional systems are susceptible to structural distortions driven by electron-phonons interactions. The most commonly studied phonons-driven instability is the metal to insulator Peierls transition in one-dimensional (1D) conductors. The insulating state is a periodic modulation of bonds charge density (BDW) associated to a lattice distortion. Such instabilities are driven by the coupling between the electrons and the inter-site phonons modes, the interaction been essentially supported by a modulation of the hopping integrals between two nearest neighbor (NN) sites. The consequence is an alternation of the bond orders while the on-site charge remains homogeneous on the whole system.

When a “site” stands for a complex system with internal degrees of freedom, there is another important type of electron-phonons (e-ph) interaction, namely the one that couples the electrons with the internal phonons modes of each “site”. This is, for instance, the case in molecular crystals where a site represents a whole molecule. In such cases the totally-symmetric (Raman active) molecular vibrational modes can couple to the system electronic structure. Holstein¹ was one of the first to understand the importance of such e-ph coupling, showing that it may lead to a self trapping of the conducting electrons by local molecular deformations. In the 60’s Little² even suggested that intra-molecular vibrations could be responsible for super-conductivity in the organic conductors. More recently it was again proposed to be the super-conductivity mediator in fullerides-based systems³.

Even-though the electron molecular-vibrations (e-mv) has now been excluded as super-conductivity mediator in organic conductors, a simple analysis shows that they should in anyway be relevant to these systems. Indeed, the conductivity-supporting molecules, such as the *TMTTF* or *TMTSF* -based molecules, the *TCNQ*-based molecules, the *M(dmit)*₂-based molecules, etc, have a certain number of characteristics in common. They are large, planar, conjugated and based on organic cycles, all characteristics favorable to a strong coupling of the conduction electrons (which, belonging to the π

conjugated system of the molecules, are strongly delocalized on the molecular skeleton) with the molecular totally symmetric (A_g) vibrational modes. This analysis is fully supported by Raman spectroscopy measurements^{4,5} which assert both the existence of low frequency vibrational modes (associated with ring angular deformations) and e-mv coupling constants belonging to the intermediate regime.

It is widely admitted that the simplest pertinent model for describing the 1D organic conductors electronic structure is the extended Hubbard (eH) model with NN bi-electronic repulsions. The present study seeks therefore at studying the combined effects of the electron correlation within the eH model and the e-mv interactions, in a quarter-filled 1D chain, relevant for organic 1D conductors. The e-mv problem have been largely addressed in the case of the one-dimensional half-filled chain⁶. Quarter-filled systems have been treated in several regimes. In the weak coupling regime renormalization group (RG) approaches⁷ show that the transition line between the Luttinger Liquid^{8,16} (LL) phase and the Luther-Emery^{9,16} (LE) phase (gaped spin channel and dominating $2k_F$ charge fluctuations) is displaced toward positive g_1 parameters when the e-mv coupling increases. In addition, the Luttinger Liquid parameters are renormalized by the e-mv interactions. In the adiabatic and small inter-site repulsion regime^{10,11}, small systems diagonalizations exhibit three different phases, one uniform phase at small e-mv coupling, associated with LL, one $2k_F$ charge density wave (CDW) phase for large enough e-mv coupling and small values of the on-site electron correlation, and one $4k_F$ CDW phase for large enough e-mv coupling and on-site repulsion. When inter-site repulsion is omitted, we have studied¹² the whole phases diagram as a function of both the phonons frequency, the e-mv coupling and the on-site correlation strength. We have shown that the dependence of the phases diagram to the phonons frequency is crucial. Indeed, while for high frequencies (corresponding to the highest A_g molecular vibrations of the Bechgaard salts) the phases diagram is very poor and well reproduced by the weak coupling approximation, for low phonons frequencies (corresponding to the lowest A_g molecular vibrations of the Bech-

gaard salts), the phases diagram is on the contrary very rich. At small e-mv coupling, and in agreement with the RG results, we found LL and LE phases with renormalized parameters. In the intermediate coupling regime, we found at surprisingly small values of the on-site repulsion (from $U/t \sim 2$), a metallic phase with dominating $4k_F$ CDW fluctuations. For large e-mv coupling we found polaronic phases where the electrons are self-trapped by the molecular deformations, either by pairs (low electron-correlation regime) or alone (large electron-correlation regime).

The NN bi-electronic repulsions are crucial for a reliable description of the 1D organic conductors. The present paper will therefore study the interplay between the e-mv and the NN bi-electronic repulsion within an extended Hubbard model. In regards to the previous results we will limit us to the low phonons frequencies where we can expect significant effects to occur.

The next section will be devoted to the model description and the computational details. Section 3 will present the results and section 4 will discuss their relevance to the organic conductor physics. The last section will conclude.

II. COMPUTATIONAL DETAILS AND MODEL

A. Model

The simplest way to couple dynamically dispersionless molecular vibrations to the electronic structure is through local harmonic oscillators and linear e-mv coupling. We will therefore use an extended-Hubbard-Holstein model (eHH). If U stands for the on-site repulsion, V for the nearest-neighbor coulomb repulsion and g for the e-mv coupling constant the eHH model can be written as $H_e + H_{ph} + H_{e-mv}$ with

$$\begin{aligned} H_e &= t \sum_{i,\sigma} (c_{i+1,\sigma}^\dagger c_{i,\sigma} + h.c.) + U \sum_i n_{i,\uparrow} n_{i,\downarrow} + V \sum_i n_i n_{i+1} \\ H_{ph} &= \omega \sum_i (b_i^\dagger b_i + 1/2) \\ H_{e-mv} &= g \sum_i n_i (b_i^\dagger + b_i) \end{aligned}$$

$c_{i,\sigma}^\dagger$, $c_{i,\sigma}$ and $n_{i,\sigma}$ are the usual creation, annihilation and number operators for an electron of spin σ located on site i ($n_i = n_{i,\uparrow} + n_{i,\downarrow}$). b_i^\dagger and b_i are the intra-molecular phonons creation and annihilation operators and ω the phonons frequency. The energy scale is fixed by $t = 1$.

As noticed in ref.¹², the on-site part of the Hamiltonian can be rewritten (apart from constant terms) as

$$\omega \left[\left(b_i^\dagger + n_i \frac{g}{\omega} \right) \left(b_i + n_i \frac{g}{\omega} \right) - n_i \frac{g^2}{\omega} + \left(U - 2 \frac{g^2}{\omega} \right) n_{i,\uparrow} n_{i,\downarrow} \right] \quad (1)$$

One may highlight the following points.

- The on-site bi-electronic repulsion term is renormalized by the e-mv coupling and the effective interaction $U_{eff} = U - 2g^2/\omega$ becomes attractive in the strong coupling regime.
- One sees from eq. 1 that the phonons and e-ph parts of the Hamiltonian can be rewritten as a displaced harmonic oscillator. The noticeable point is that the displacements are proportional to the sites charge, simulating this way the relaxation of the molecular geometry as a function of the ionicity of the site.
- The natural basis for the phonons states is therefore the eigenstates of the displaced oscillators. Such a vibronic representation is not only very physical, but also particularly suited for the representation of the low energy physics. Despite the fact that one would have a complete basis set for each value of the sites occupation, the necessity to work in a truncated representation lift the problem of over-completeness.
- One should also notice that there is a strong renormalization of the hopping integrals between the initial and final vibronic states of two neighboring sites, by the Franck-Condon factors. In this representation the Franck-Condon factors correspond to the overlaps between the vibronic states associated with ± 1 occupation numbers. As physically expected, when an electron hops between two sites vibronic ground states, the hopping integral is exponentially renormalized by the displacement : $t \rightarrow t \exp \left[- (g/\omega)^2 \right]$. The direct consequence is an increased tendency to electron localization. Indeed, vibronic high energy states need to be summed up for delocalization processes when the e-mv coupling is large.
- The pertinent e-mv coupling parameter is not g but rather g/ω , in the light of which it becomes clear that only vibrations of low frequencies may produce significant effects other than a simple renormalization of the pure electronic interactions. The model pertinent parameters are therefore U/t , V/t , ω/t and g/ω

B. Computational details

The calculations have been carried out using the infinite system density-matrix renormalization group (DMRG) method¹³ with open boundary conditions.

Since an infinite number of phononic quantum states lives on each site we have truncated the phonons basis set according to the previous section analysis, that is we kept only the two lowest vibronic states on each site (i.e. the two lowest eigenstates of the on-site Hamiltonian). This choice is physically reasonable since (i) we work at $T = 0$

and therefore only the lowest vibronic states are expected to be involved, (ii) the molecules form well defined entities that are only perturbatively modified by the presence of their neighbors. As already mentioned, when an electron hops between two nearest neighbors sites the hopping integral is renormalized by the Franck-Condon factors, i.e. the overlap between the initial and final vibronic states of the sites, $\langle (n, \nu, Sz)_i ; (n', \nu', Sz')_{i+1} | H | (n-1, \mu, Sz \pm 1/2)_i ; (n'+1, \mu', Sz \mp 1/2)_{i+1} \rangle = t \langle \nu | \mu \rangle \langle \nu' | \mu' \rangle$ (n and n' being the number of electrons on sites i and $i+1$ respectively, ν and μ , ν' and μ' the phonons states and Sz , Sz' the spin projection quantum numbers). Figure 1 shows the overlap between the vibronic ground state of a site supporting n electrons and the vibronic states of the same site supporting $n \pm 1$ electrons. As can be seen, when g/ω is small the overlap, and therefore the Franck-Condon factor, decreases very quickly with the number of bosons, thus only the first few vibronic states are involved and the truncation is totally pertinent. This fact is confirmed by exact calculations on small systems (4 sites) where four phononic quantum numbers have been considered. For instance, the weight of the 3 and 4 bosons contributions in the wave functions is only 0.012 for $g/\omega = 0.5$, $U/t = 4$ and $U/V = 4$. When g/ω increases, the maximum of the Franck-Condon factors is rapidly displaced toward very large number of bosons. These vibronic states being strongly hindered by their large vibrational energy, they have a small weight in the wave function and the system tends to localize. For instance for $g/\omega = 3$, $U/t = 4$ and $U/V = 4$, the weight of the 3 and 4 bosons contributions in the 4 sites system is only 1.2×10^{-3} . In the intermediate region the contribution of intermediately large phonons states (with occupations 3, 4, 5) is not as negligible (0.3 for $g/\omega = 1.5$, $U/t = 4$ and $U/V = 4$), and the basis set truncation lowers the total hopping between nearest neighbors sites and thus increases the system localization. One can therefore expect that in the intermediate regime the true phases transitions will be displaced — compared to our results — toward larger values of the electron-phonon interaction. It is however clear that any truncated basis set will have a great deal of problem to accurately treat systems too close to a phases transition since the effective softening of the frequency near the transition translates into the implication of a quasi-infinite number of phonons states. From the above analysis, one can be quite confident in the quality of the numerical results and in particular in the different phases found in this work, provided that the exact position of the transitions is not seek at, in the intermediate coupling region. In order to estimate more precisely the transition displacement due to the basis set truncation, we have run additional calculations using up to three bosons states per site occupation number (that is 12 on-site states) for a set of chosen electronic parameters ($U/t = 4$, $U/V = 4$) and all values of the electron-phonon coupling constant.

In order to characterize the phases diagram, we have

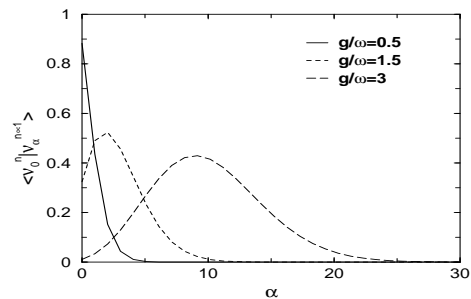


FIG. 1: Overlap between the vibronic ground state ν_0^n of a site supporting n electrons and the α^{th} vibronic state $\nu_\alpha^{n \pm 1}$ of a site supporting $n \pm 1$ electrons .

computed the charge and spin gaps, defined as usual :

$$\Delta_\rho = E_0(2N, N+1, 0) + E_0(2N, N-1, 0) - 2E_0(2N, N, 0)$$

and

$$\Delta_\sigma = E_0(2N, N, 1) - E_0(2N, N, 0)$$

where $E_0(N_s, N_e, Sz)$ is the ground state (GS) energy of a system of N_e electrons, N_s sites and spin projection Sz . In addition, we have computed the charge-charge, spin-spin correlation functions : $c_A(j) = \langle (A_0 - \langle A_0 \rangle) (A_j - \langle A_j \rangle) \rangle$ where A stands either for the number operator, n , or for the spin projection operator, Sz , and the on-site singlet correlation function : $c_{Sg}(j) = \langle Sg_0^\dagger Sg_j \rangle$ where $Sg_i^\dagger = c_{i,\uparrow}^\dagger c_{i,\downarrow}^\dagger$ and Sg_i are the singlet creation and annihilation operators on a site.

The properties calculation have been computed using 255 states per renormalized block, whereas for the gaps calculations we have used a double extrapolation (i) on the systems size, and (ii) on the number, m , of states kept, using $m = 100, 150$ and 255. In all calculations we have computed systems of size up to 80 sites and extrapolated to the infinite chain.

To have more information on the localized phases wave functions we have also computed the density matrices at the central sites and performed exact diagonalization of small systems.

III. RESULT

The present work explores the whole range of the on-site repulsion strength and of the e-mv coupling. The vibration frequency have been chosen to be $\omega/t = 0.2$ for the reasons already exposed in the preceding paragraphs. The phases diagrams have been computed for two values of the nearest-neighbor versus on-site repulsions ratio V/U which are recognized to be generic for the 1D organic conductors¹⁴, namely $V = U/4$ and $V = U/2$.

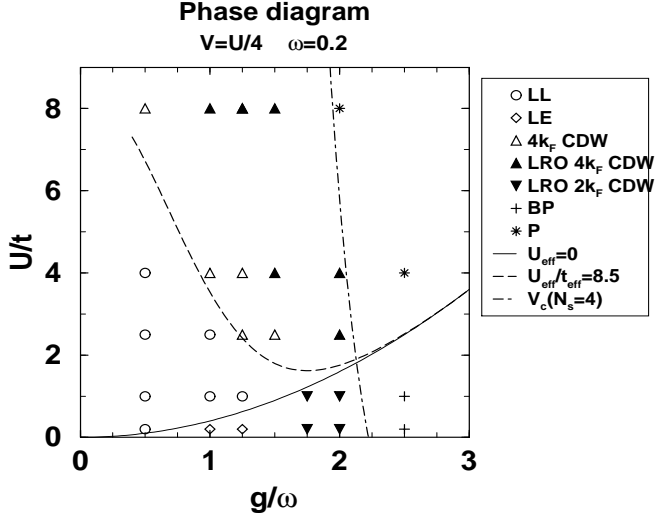


FIG. 2: Phases diagram of the extended Hubbard-Holstein model for $V = U/4$ and $\omega/t = 0.2$.

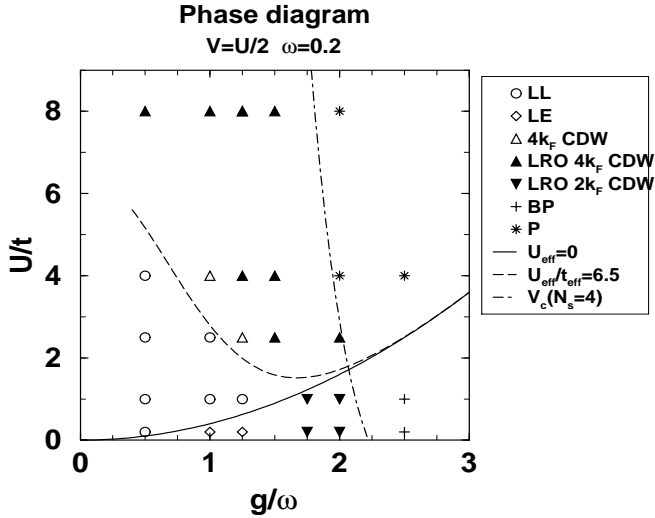


FIG. 3: Phases diagram of the extended Hubbard-Holstein model for $V = U/2$ and $\omega/t = 0.2$.

Figure 2 and 3 report the phases diagrams for $V = U/4$ and $V = U/2$ as a function of g/ω and U/t . The two diagrams present the same general features with seven different phases. The major effect of the introduction of NN repulsion in the Hubbard-Holstein model is to stabilize two new phases in the e-mv intermediate coupling regime. From another point of view, the inclusion of the e-mv coupling in the extended Hubbard model has similar consequences as its inclusion in the pure Hubbard model; that is : the apparition of polaronic and bi-polaronic phases in the strong coupling regime, the apparition of a $4k_F$ CDW phase in the intermediate regime for extremely low values of the on-site repulsion.

To summarize, in the weak coupling regime one find both the Luttinger Liquid phase for $U_{eff} > 0$ and the Luther Emery phase for $U_{eff} < 0$. In the strong coupling

regime one has the polaronic ($U_{eff} > 0$) and bi-polaronic ($U_{eff} < 0$) phases where the electrons are self-trapped (alone or by pairs) by the molecular geometry deformations. In between these two regimes, that is for intermediate e-mv coupling, one finds the two new phases. The first one is an insulating long-range ordered $4k_F$ CDW phase which develops at the extend of the metallic $4k_F$ CDW phase for $U_{eff} > 0$. The second one is an insulating long-range ordered $2k_F$ CDW phase which develops for $U_{eff} < 0$ at the expends of the localized bi-polaronic phase. It is noticeable the $U_{eff} = 0$ line seems to remain a strict phases boundary. On the contrary the other frontiers have been shifted. For $U_{eff} > 0$ the localized phases are enhanced and the delocalized ones reduced. On the contrary, for $U_{eff} < 0$ the bi-polaronic phase is reduced.

A. The $U_{eff} > 0$ phases

1. Luttinger liquid phase

For small values of g/ω , up to intermediate ones if the on-site repulsion U is not too large, one finds, both in the $U/V = 4$ and $U/V = 2$ cases, the expected LL phase. The computed charge and spin correlation functions exhibit power law behavior with dominant $2k_F$ SDW fluctuations and sub-dominant CDW fluctuations. The spin and charge gaps extrapolate nicely to zero to numerical accuracy.

Similarly to what happens in the pure extended Hubbard model¹⁵, the $2k_F$ SDW fluctuations and the $4k_F$ CDW fluctuations are enhanced by increasing values of the NN repulsions. From the charge structure factor

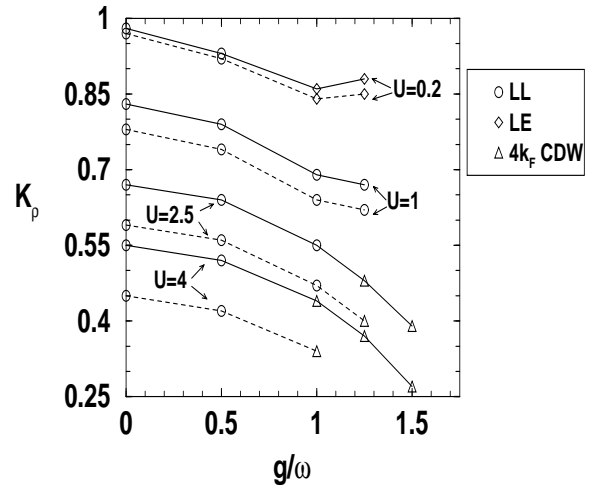


FIG. 4: K_ρ as a function of g/ω for $U = 0.2, 1, 2.5, 4$, $V = U/4$ (solid lines) and $V = U/2$ (dashed lines). The symbols follow the same pattern as in the phases diagrams.

$S_\rho(q)$ we have computed the LL K_ρ parameter as

$$K_\rho = \pi \left. \frac{d}{dq} S_n(q) \right|_{q=0}$$

Figure 4 reports the K_ρ parameter as a function of both U/V and g/ω . Once again the results are a simple superposition of the K_ρ reduction effect due to the NN repulsions and the reduction effect due to the e-mv coupling.

2. The $4k_F$ CDW phase

The LL phase is bordered, both for $V = U/4$ and for $V = U/2$, by a metallic phase presenting dominating $4k_F$ charge fluctuations. This phase have very similar characteristics as the $4k_F$ CDW phase found for $V = 0$ ¹², that is no charge neither spin gap (to numerical accuracy), power law decreasing of the charge and spin correlation functions, dominant $4k_F$ CDW fluctuations and very small values of K_ρ compared to the purely electronic model. One has for instance, for $U/t = 4$ and $V/t = 1$, $K_\rho = 0.28$ when $g/\omega = 1.5$ instead of $K_\rho = 0.55$ in the pure electronic eH model (see fig. 4). One should however notice that while the K_ρ values remain always larger than the $1/4$ minimal value predicted by the LL theory¹⁶ for metallic behavior, it can be as large as 0.48 for $U = 2.5$, $g/\omega = 1.25$ and $V = U/4$, that is much above the $1/3$ limiting value predicted by the LL theory for dominant $4k_F$ CDW fluctuations¹⁶. Despite the absence of long range coulombic repulsions, this phase is in fact, in many ways very alike a Wigner crystal.

Figures 2 and 3 show that the NN repulsions have a strongly destructive effect on this phase. Indeed, it reduces strongly its domain of existence for increasing g/ω . Compared to the $V = 0$ case a new insulating, long-range order (LRO) $4k_F$ CDW phase has taken a large part of the g/ω parameters range of the metallic $4k_F$ CDW phase. For increasing V/U the metal to insulator phases transition (MIT) is repelled to smaller values of g/ω , squeezing the metallic $4k_F$ CDW phase toward the LL one.

3. The LRO $4k_F$ CDW phase

As g/ω increases, the system undergoes a metal to insulator phases transition and the $4k_F$ CDW fluctuation phase condensates into a long range ordered $4k_F$ CDW phase.

In order to characterize this new phase, we have computed the staggered charge correlation functions $(-1)^j \mathcal{C}_n(j)$ where

$$\mathcal{C}_n(j) = \langle (n_i - \bar{n})(n_{i+j} - \bar{n}) \rangle$$

and $\bar{n} = N_e/N_s = 1/2$ is the average charge per site. The

associated order parameter is therefore

$$X_{4k_F} = \lim_{N_s \rightarrow +\infty} \sum_j (-1)^j \mathcal{C}_n(j)$$

In this gaped regime, one should be careful and clearly distinguish between the correlation functions $\mathcal{C}_n(j)$ and the correlation functions of the observable fluctuations $c_n(j)$. Indeed, while in delocalized phases the two do not differ, in gaped phases the correlation functions tends toward a non zero constant as the inter-site distance increases, while the fluctuations decrease quickly to zero at infinite inter-site distances¹⁶.

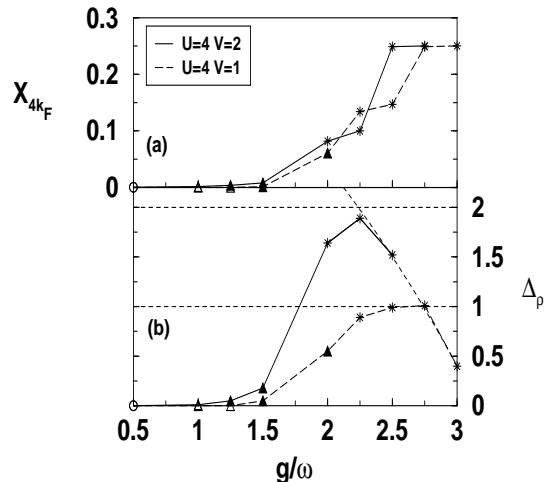


FIG. 5: (a) Order parameter X_{4k_F} and (b) charge gap as a function of g/ω for $U = 4$. The solid lines correspond to $U/V = 2$ and the long dashed lines to $U/V = 4$. The symbols follow the same pattern as in the phases diagrams. The short light dashed lines correspond respectively to $\Delta_\rho = V$ (that is $V = 2$ and $V = 1$) and $\Delta_\rho = U_{eff}$.

Figure 5 reports both the charge gap Δ_ρ and the order parameter X_{4k_F} as a function of g/ω , for the two values of the NN repulsion. One sees immediately that the opening of the charge gap from the metallic $4k_F$ CDW phase is simultaneous with the formation of the long range order. Similarly the computed charge fluctuations correlation functions $c_n(j)$ go from a power law behavior as a function of increasing inter-site distances to an exponential behavior. One should note that the spin channel remains ungaped and the corresponding fluctuations correlation functions $c_{S_z}(j)$ decrease as a power law with increasing inter-site distances.

At the metal to insulator phases transition, that is for intermediate values of g/ω ($\simeq 1$), one observes a smooth opening (exponential like) of both the charge gap and the order parameter ; opening that seems consistent with a Kosterlitz-Thouless transition. For large value of g/ω , the order parameter saturates and the system undergoes a self-trapping transition of the electrons toward a polaronic phase. It is noticeable that, while the MIT is very

soft, the self-trapping transition is on the contrary rather sharp.

4. The small polaronic phase

As expected from previous works^{1,12,17,18}, in the strong coupling regime but still positive effective on-site repulsion, $U_{eff} = U - 2g^2/\omega$, the system undergoes a transition toward a polaronic phase where the electrons are self-trapped by the molecular distortions. This trapping is mediated by the Franck Condon factors, that strongly renormalize the hopping integrals between low energy vibronic states. One can remember that the hopping between the ground vibronic states is renormalized as $t \rightarrow t_{eff} \sim t \exp(-(g/\omega)^2)$. The ground state of the system is therefore dominated by configurations such as :

$$..10101010..$$

where the 1 stand for sites supporting one electron and the 0 stand for empty sites. The validity of this picture has been checked both on the GS wave function of small systems (4 and 8 sites, PBC, exact diagonalization) and the on-site density matrix in the DMRG calculations. On small systems the computed weight of those configurations is always larger 0.85 with, for instance, 0.900 for $U = 4$, $V = 2$, $g/\omega = 2$ and 4 sites. On large systems, we have computed the central sites density matrices and found that the probability of having double occupations is extremely small, with for instance, $\rho(\uparrow\downarrow) \leq 10^{-9}$ for $U = 4$, $g/\omega = 2.5$ and all values of U/V . Coherently, the GS energy per site is nearly independent of the system size and verify — up to at least 4 significant numbers — on all the computed points, the formula $-N_e/N_s g^2/\omega + \omega/2$. Such a GS is strongly quasi-degenerated due to the equivalence between the odd and even sites and the different spin configurations. The small splitting is due to the residual delocalization and therefore scales as $t_{eff} = t \exp(-(g/\omega)^2)$ (see figure 6). The spin channel remains ungaped. The main difference between the present phase and the phase found in the HH model stays in the charge channel. Indeed, the NN repulsion is responsible for the opening of a strong gap (see figure 5) that did not exist in the $V = 0$ case. In fact, the charge gap scales as the cost to add an extra electron to the system. In the case of open systems the end sites being always occupied, Δ_ρ scales as $\min(U_{eff}, V)$ (according to whether the extra electron is located on an “empty” site or on an already “occupied” one) while in periodic systems is scales as $\min(U_{eff}, 2V)$. The change of behavior in Δ_ρ can be clearly seen on figure 5, where, for instance, the gap for $U = 4$, $U/V = 4$ undergoes a saturation to $\Delta_\rho = V = 1$ at the self-trapping transition (that occurs between $g/\omega = 2$ and $g/\omega = 2.2$) and then a strong decrease for $g/\omega \geq \sqrt{15}/2 \simeq 2.74$ ($U_{eff} = V$), where it behaves as $U - 2g^2/\omega$. One should notice that the full saturation of the order parameter occurs only after the second transition.

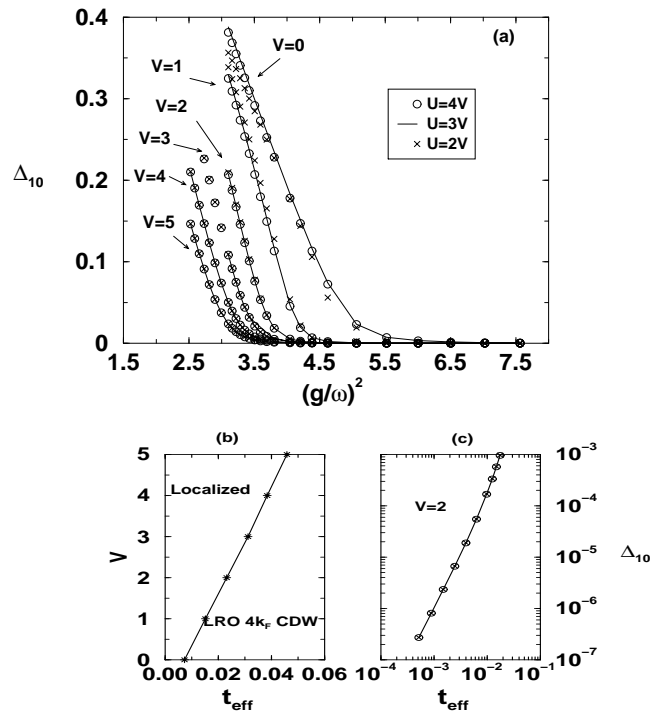


FIG. 6: (a) First excitation energy, Δ_{10} , as a function of g^2/ω^2 for 4 sites systems, several value of V and for $U = 4V$ (circles), $U = 3V$ (solid lines) and $U = 2V$ (crosses). For the $V = 0$ case we have chosen $U = 8$, $U = 4$ and $U = 2$. (b) Phase boundary between the $4k_F$ LRO CDW phase and the polaronic phase as a function of V and t_{eff} . (c) Δ_{10} as a function of t_{eff} in a log-log curve for small values of t_{eff} (for clarity, we only show the curves for $V = 2$).

In order to better study the position of the phases transition between the $4k_F$ LRO CDW and the polaronic phase, we performed exact diagonalizations on periodic small systems (4 sites, 2 electrons). One should remember that while the $4k_F$ LRO CDW phase has a non-degenerated GS, the polaronic phase presents a quasi-degenerated GS, the degeneracy lifting being of the order of magnitude of t_{eff} . We have therefore used the first excitation energy, Δ_{10} , as a criteria for the phases transition. Figure 6(a) reports Δ_{10} as a function of g^2/ω^2 for different values of U and V . One first notice that the excitation energies depend in a negligible way on on-site repulsions. On the contrary it does strongly depend on the NN repulsion. Going from very large e-mv coupling to smaller values, the excitation energy first increases as a power law of $t_{eff} = t \exp(-g^2/\omega^2)$ (see figure 6(c)) in the polaronic phase then linearly as a function of g^2/ω^2 in the $4k_F$ CDW LRO phase. Decreasing g^2/ω^2 to even lower values this excitation energy should go through a maximum and then decrease back to zero at the MIT. The location of the phases transition between the $4k_F$ LRO CDW and the polaronic phase have been evaluated as the point where the linearly extrapolated excitation energy

of the $4k_F$ LRO CDW phase crosses the zero axis. Figure 6(b) reports the phase boundary as a function of t_{eff} and V . One sees immediately that it follows a perfectly linear curve that can be fitted as $V = 129.36t_{eff} - 0.93t$, in these coordinates. This curve have been reported on the phases diagrams (figures 2 and 3) as the V_c curves. One sees immediately that the phases transition position is very weakly dependent of the system size (as expected from such localized systems) and that the small systems estimations work pretty well for the infinite systems.

B. The $U_{eff} < 0$ phases

1. The Luther-Emery phase

For negative values of U_{eff} and small values of g/ω , we found a metallic phase for which all spin, charge and on-site singlet fluctuations correlation functions decrease with the inter-site distances, as power law. All three correlation functions exhibit dominating $2k_F$ components. In all computed cases, the $2k_F$ CDW fluctuations have the largest amplitudes. The main effect of the NN repulsion is to increase the amplitude of the CDW fluctuations and to strongly decrease the amplitude of the on-site singlet fluctuations. The charge gaps clearly extrapolate to zero, whereas we found a very small gap in the spin channel ($\Delta_\sigma \sim 0.002 - 0.003$). This fact is not incompatible with the behavior of the spin-spin correlation function, since very small gaps means very large correlation lengths of the order of magnitude of Δ_σ^{-1} . The expected exponential behavior of the spin correlation functions should therefore take place at inter-site distances larger than the computed chain lengths. One can easily recognize in this phase a weakly gaped Luther-Emery phase. The values of K_ρ extracted from the charge structure factors are strongly reduced compare to the values of the purely electronic model, in a similar way as what has been found in the $V = 0$ case. It should be noted that K_ρ always remains lower than 1 in agreement with dominant CDW fluctuations.

2. The LRO $2k_F$ phase

When g/ω increases toward the intermediate regime ($g/\omega > 1.5$), the system undergoes a MIT toward an insulating phase presenting a $2k_F$ long range order. One should notice that this phase is induced by the NN repulsions and does not exist in the Hubbard Holstein model. In comparison to the $V = 0$ case, the $2k_F$ LRO phase develops at the expense of the bi-polaronic phase. It is interesting to point out that for positive U_{eff} the development of the $4k_F$ LRO phase, induced by the NN repulsions, have a tendency to localize the electronic structure, while for negative U_{eff} , the development of the $4k_F$ LRO phase corresponds to a tendency toward a less localization. The amplitude of the charge correlation functions

$\mathcal{C}_n(j)$ extrapolate at infinite inter-site distances toward finite values (for instance 0.06 for $U = 1$, $V = 0.5$ and $g/\omega = 2$). The order parameter has been defined in the usual way

$$X_{2k_F} = \lim_{N_s \rightarrow +\infty} \left| \sum_j e^{i2k_F j} \mathcal{C}_n(j) \right|$$

and is reported on figure 7. One can see that, as in the $4k_F$ LRO phase, the order parameter increases very slowly at the MIT as in a Kosterlitz-Thouless transition.

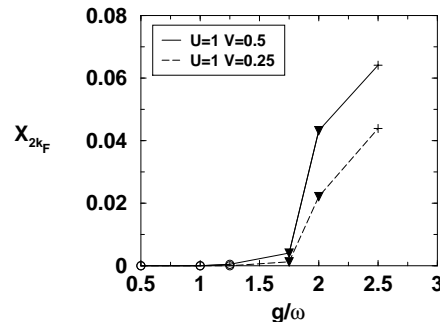


FIG. 7: Order parameter X_{2k_F} as a function of g/ω for $U = 1$. The solid lines correspond to $U/V = 2$ and the long dashed lines to $U/V = 4$. The symbols follow the same pattern as in the phases diagrams.

Both spin and charge channels are gaped. It is noticeable that the gaps values are always of the same order of magnitude : $\Delta_\rho = \Delta_\sigma = 1.04$ for $U = 0.2$, $V = 0.1$ and $g/\omega = 2$, $\Delta_\rho = 0.35$, $\Delta_\sigma = 0.33$ for $U = 1$, $V = 0.25$ and $g/\omega = 2$. Coherently, the fluctuations correlation functions (spin, charge and on-site singlet) decrease exponentially with the inter-site distances (see figure 8).

One should note that, for large $|U_{eff}|$, the on-site singlet fluctuations correlations are dominant, whereas, for weak $|U_{eff}|$, the charge fluctuations correlations dominate. On the contrary the increase of V , increases the CDW at the expense of the singlet fluctuations.

3. bi-polaronic phase

For large values of g/ω the system goes in a bi-polaronic phase where the attractive nature of the effective on-site interaction strongly couples the electrons in pairs. This pairing is associated with a strong localization and a self-trapping of the pairs, due to the rescaling of the hopping integrals between low energy vibronic states by Franck Condon factors. The remaining delocalization processes are very small and the ground state wave functions have dominant configurations of the type

..20002000..

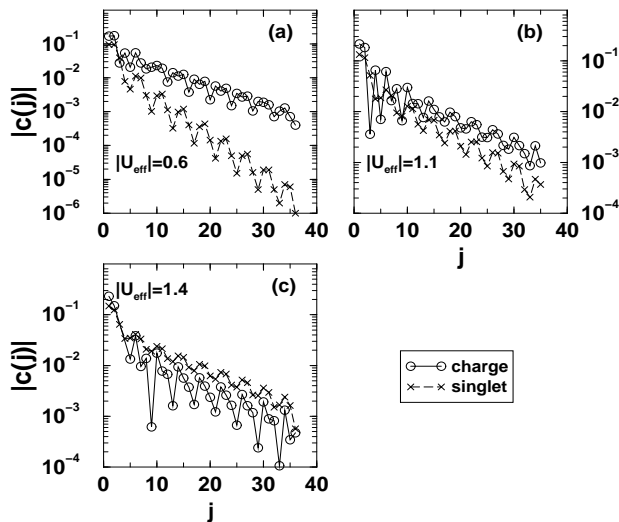


FIG. 8: Charge (circles) and singlet (crosses) fluctuations correlation functions for $U/V = 2$, $g/\omega = 2$ and different values of U_{eff} . $U_{\text{eff}} = 0.6$ (a), $U_{\text{eff}} = 1.1$ (b) and $U_{\text{eff}} = 1.4$ (c).

where 2 stands for a double occupancy of a site and 0 for an empty site. The probability of having a lonely electron on a site is extremely small with for instance values smaller than 10^{-7} for $U/t = 1$, $V/t = 0.25$ and $g/\omega = 2.5$. The energy per site is nearly constant and in excellent agreement with the formula $1/4 U_{\text{eff}} - 1/2 g^2/\omega + 1/2 \omega$ (the difference between the computed values and the formula being of the order of 10^{-5} for $U/t = 1$, $V/t = 0.25$ and $g/\omega = 2.5$). Let us notice that the GS is strongly quasi-degenerated due to the equivalence between the four different phases of the CDW and to the absence of second neighbors repulsion terms. As in the polaronic phase the degeneracy splitting scales as t_{eff} . Finally the system is strongly gaped both in the charge and spin channels. Indeed, either to extract an electron from the system or to build a triplet state, one needs to break an electron pair. Such a mechanism cost the energy U_{eff} and therefore both gaps scale as it.

C. The basis set truncation effect

As we already mentioned the phononic basis set truncation to two vibronic states per occupation number should induce a bias toward excessive localization in the intermediate regime. This is precisely the range of coupling parameters where the new phases appears and, as we will see later, the coupling regime which is the most interesting for the physics of real systems. In order to quantify the effects of the basis set truncation we have performed, in addition to the small systems calculations presented in section II B, infinite system DMRG calculations with three vibronic states kept for each site occupation and spin. Each site is then described by twelve

states instead of eight. Since these calculations are very expensive we have only performed them for a fixed set of electronic parameters $U/t = 4$ and $V/U = 1/4$. Varying the electron-phonons coupling parameter therefore leads us to go from the Luttinger Liquid phase up to the polaronic phase. Figure 9 reports the order parameter X_{4k_F} for the two and three phonons states. As expected

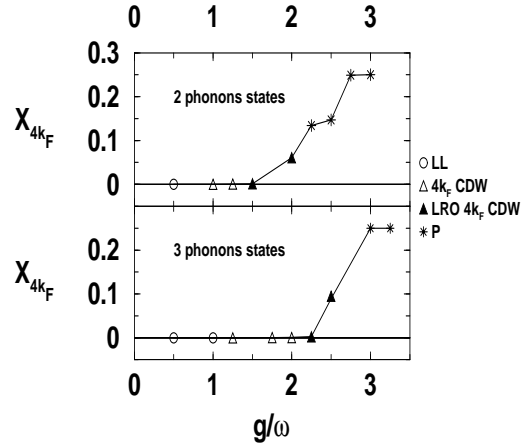


FIG. 9: X_{4k_F} order parameter for two (upper curve) and three (lower curve) phonons states kept per electronic state on each site. The phases symbols follow the same pattern as in the phases diagrams.

the increase of the basis set results in a displacement of the phases transitions toward larger value of the coupling constant, that is a larger delocalization of the system for a given value of g/ω . The Luttinger Liquid phase is only slightly enlarged, in agreement with the weak participation of excited vibronic states in the small systems wave functions. The phase which is the most favored by the basis set increase is the metallic $4k_F$ CDW phase. Indeed this phase is substantially extended toward larger values of g/ω while the insulating LRO $4k_F$ phase is essentially translated by $0.75g/\omega$.

In conclusion the basis set truncation does not change the structure of the phases diagram, its main effect being of reducing the range of the metallic $4k_F$ CDW phase, essentially on the side of the larger values of the electron-phonons coupling parameter, and shifting the LRO $4k_F$ phase toward smaller values of g/ω . All these results are in complete agreement with the small system calculations.

IV. RELEVANCE TO THE ORGANIC CONDUCTORS PHYSICS

In this section we are going to discuss the pertinence of the above calculations for the low energy physics of organic conductors and more specifically for

the $(DX - DCNQI)_2 M$ family and the Bechgaard salts family. Indeed, as already mentioned in the introduction, the building molecules of these systems present a certain number of similar characteristics that are crucial for the relevance of the molecular vibrations to the electronic structure. The $DX - DCNQI$ as well as the $TMTTF$ or $TMTSF$ molecules are planar, strongly conjugated and their skeleton is based on organic cycles ; the quinone cycle for the $DX - DCNQI$ and the two pentagonal cycles of the fulvalene for the $TMTTF$ and $TMTSF$. These geometrical properties strongly favor the existence of low frequency vibrational modes, namely the angular distortion of the cycles, the bond length remaining untouched. Among these, the A_g modes couple to the electronic structure in a relatively strong manner, leading to e-mv coupling constants in the intermediate range (as can be seen in Raman experiments⁴ or in the geometry relaxation of the molecules with their ionization¹⁹). In addition, one should notice that due to their conjugated character, the π system of the considered molecules are strongly delocalized on their skeleton and thus strongly polarizable. The consequence is that the second neighbor coulombic interactions should be strongly screened by the “metallic plate” of the in-between molecule. One can therefore reasonably assume that the on-site and first neighbor repulsion terms are the only pertinent ones for the physics of these organic 1D systems.

Recently charge ordered phases presenting similar characteristics with the $4k_F$ LRO CDW state have been observed both in the $(DX - DCNQI)_2 M$ family and in the Bechgaard salts family.

The most characteristic compound is certainly the $(DI - DCNQI)_2 Ag$ compound. Indeed, this system which is strongly one dimensional undergoes a MIT phases transition at 220K toward a $4k_F$ CDW state²⁰. Both NMR²¹ and X-ray²² show that the insulating state exhibit a on-site charge disproportionation between two adjacent molecules. This charge order saturates at a 3 : 1 ratio below 140K and is associated with a molecular geometry deformation due to the ionicity modification. In addition, the spin channel remains ungaped²¹. This compound, which is usually considered as strictly non-dimerized (despite a recent doubt raised by Meneghetti *et al*²³) seems to be the perfect example of an e-mv driven $4k_F$ LRO CDW state as the one discussed in this paper. Most authors assume that this LRO state is driven by a Wigner crystallization due to strong long range electronic repulsions. We have seen in the previous sections, that the e-mv driven $4k_F$ CDW phases present very similar characteristics as the Wigner crystals, without the need of very strong correlation effects and without long range repulsions. In the light of the previous considerations on the strongly polarizable electronic structure of the quinone cycles, on the usually assumed values of the electronic correlation strength (in the intermediate range rather than the strong range for the $DCNQI$ family²⁴), and on the e-mv coupling characteristics, it seems to us more plausible that the considered $4k_F$ CDW

state is driven by the e-mv than by the usual unscreened strong coulombic repulsions. At very low temperatures the $(DI - DCNQI)_2 Ag$ undergoes a second phases transition toward a spin ordered state where the $4k_F$ LRO CDW is associated with a $2k_F$ anti-ferromagnetic LRO. These results are in agreement with the $2k_F$ SDW fluctuations exhibited in the $4k_F$ LRO CDW phase of the eHH model, fluctuations that could easily be pinned at low temperatures by impurities or inter-chains interactions.

Another family for which the preceding analyses are relevant about the e-mv influence on the electronic structure, is the Bechgaard salts family. This fact should be put in the light of the newly discovered $4k_F$ charge ordered phase. This phase have been observed on several systems such as in the $(TMTTF)_2 PF_6$ or the $(TMTTF)_2 AsF_6$ ²⁵. The charge ordered (CO) phase appears when the temperature is lowered from the metallic Luttinger Liquid phase through a soft cross over. It is noticeable that transport measurements observe $4k_F$ CO fluctuations in the normal LL phase, indicating that the interactions driving the transition are relevant far inside the normal phase and over a large range of pressures^{26,27}. X-ray diffraction measurements do not see any n-merization associated with this phases transition, excluding a Peierls mechanism. NMR measurements on the carbon atoms of the central double bond of the fulvalene (on which the Highest Occupied Molecular Orbital, responsible for the low energy physics of these systems, have large coefficients) exhibit a charge disproportionation on NN molecules. Magnetic susceptibility measurements are transparent to this phases transition and the spin channel remain ungaped. It is clear that all these experimental results are in full agreement with the characteristics found in the present work for the $4k_F$ LRO phases transition. Despite the fact that the system dimerization has not been taken into account in the present work, the e-mv coupling appears as a strong candidate for the CO driving mechanism. It is however clear that the dimerization degree of freedom should be taken into account, in addition to the correlation degrees of freedom (both on-site and inter-sites) and the e-mv degrees of freedom treated in the present work, for a complete description of the Bechgaard salts.

Finally, one can point out that the mechanism underlying a MIT transition toward an on-site charge modulation, driven by the e-mv, does not imply any lattice distortion apart from small modifications in the molecular geometries, in particular in the angles of the cycles (the fulvalene cycles in the Bechgaard salts). Indeed such geometrical relaxations can be expected to be a consequence of the charge disproportionation. These transitions should therefore be $q = 0$ transitions.

V. CONCLUSION

The present paper studies the influence of the electron-molecular vibration coupling on the electronic structure

of correlated 1D quarter-filled chains. The model chosen is the extended-Hubbard Holstein model, that is the simplest one containing both electron correlation effects relevant for the physics of molecular crystals such the organic conductors, and e-mv coupling whose effects can be expected to play a crucial role. We have found that for low phonons frequencies the electronic structure is strongly affected by the presence of molecular vibrations. One of the most striking results being the existence of $4k_F$ CDW phases, one metallic and one insulating charge ordered phase, for small values of the correlation strength (as small as $U/t = 2$), small values of the nearest neighbor repulsion and in the absence of long range coulombic repulsion. A study of these phases shows however that they have similar characteristics as a Wigner crystal. In this light a new interpretation — based on the e-mv coupling — of the origin of the $4k_F$ charge ordered phase in the $(DI-DCNQI)_2Ag$ and of the recently discovered CO phase in the $(TMTTF)_2X$ family has been proposed. Such an interpretation of the apparition of the $4k_F$ CO phase present the advantage over the usual purely elec-

tronic interpretation to be in agreement with the usual values of the correlation strength for these systems and the strong screening of the long range bi-electronic repulsions that can be expected from the π conjugated character of the building molecules. To conclude we would like to point out that for a complete description of the Bechgaard's salts physics, one should treat in addition to the intra-molecular phonons modes, the inter-molecular modes responsible for the known dimerization in these compounds. In view of the recent work of Campbell, Clay and Mazumdar²⁸ on the adiabatic dimerized extended-Hubbard Holstein model that forecasts the existence of mixed phases such as the Bond Charge Density Wave and the Spin-Peierls $4k_F$ CDW phase, it would be of interest to conduct the same type of study as the present one on the dimerized extended-Hubbard Holstein model. Indeed, such a model would include all degrees of freedom important for 1D organic conductors as well as the phonons quantum fluctuations that have been proved to be crucial for a correct description of the e-mv coupling²⁹

-
- * Electronic address: Marie@irsamc.ups-tlse.fr
- ¹ T. Holstein, Ann. Phys. **8**, 325 (1959).
 - ² W. A. Little, Phys. Rev. **134**, A1415 (1964).
 - ³ A.S. Alexandrov, V.V. Kabanov, Phys. Rev. **B 54**, 3655, (1996).
 - ⁴ M. Meneghetti, R. Bozio, I. Zanon, C. Pelice, C. Ricotta, M. Zanetti, J. Chem. Phys. **80**, 6210 (1984).
 - ⁵ T. Ishiguro, K. Yamaji, and G. Saito, in *Organic Superconductors*, 2nd ed., Springer Series in Solid-State Sciences, Vol. 88 (Springer-Verlag, Berlin, 1998) ; C. Bourbonnais and D. Jerome, in *Advances in Synthetic Metals, Twenty Years of Progress in Science and Technology*, ed.by P. Bernier, S. Lefrant, and G. Bidan (Elvesier, New York, 1999).
 - ⁶ J.E. Hirsch, Phys. Rev. **B 31**, 6022, (1985).
 - ⁷ J. Voit and H. J. Schulz, Phys. Rev. **B 37**, 10068 (1988) ; J. Voit, Phys. Rev. Letters **64**, 323 (1990).
 - ⁸ F.D.M. Haldane, J. Phys. C **14**, 2585 (1981)
 - ⁹ A. Luther and V.J. Emery, Phys. Rev. Lett. **33**, 589 (1974)
 - ¹⁰ J. Riera and D. Poilblanc, Phys. Rev. **B 59**, 2668 (1999).
 - ¹¹ K. C. Ung, S. Mazumber and D. Toussaint, Phys. Rev. Lett. **73**, 2603 (1994).
 - ¹² P. Maurel and M. B. Lepetit, Phys. Rev. **B 62**, 10744 (2000).
 - ¹³ S. R. White, Phys. Rev. Lett. **69**, 2863 (1992) ; S. R. White, Phys. Rev. **B 48**, 10345 (1993).
 - ¹⁴ A. Fritsch and L. Ducasse, J. Physique I **1** (1991) 855 ; F. Castest, A. Fritsch and L. Ducasse, J. Physique I **6** (1996) 583.
 - ¹⁵ J. E. Hirsch and D. J. Scalapino, Phys. Rev. **B 27**, 7169 (1983) ; *ibid* Phys. Rev. **B 29**, 5554 (1984).
 - ¹⁶ J. Voit, Rep. Prog. Phys. **58**, 977 (1995).
 - ¹⁷ A.S. Alexandrov, V.V. Kabanov and D.K. Ray, Phys. Rev. **B 49**, 9915 (1994).
 - ¹⁸ M. Capone, M. Grilli and W. Stephan, J. Supercond., **12**, 75 (1999).
 - ¹⁹ J.R. Andersen, K. Bechgaard, C.S. Jacobsen, G. Rindorf, H. Solig and N. Thorup, Acta Crystallogr. sect. B, **B 34**, 1901 (1978) ; T.J. Kistenmacher, T.J. Emge, P. Shu and D.E. Cowan, Acta Crystallogr. sect. B, B35, 772 (1979).
 - ²⁰ K. Hiraki and K. Kanoda, Phys. Rev. **B 54**, R17276 (1996).
 - ²¹ K. Hiraki and K. Kanoda, Phys. Rev. Letters **80**, 4737 (1998) ; K. Kanoda, K. Miyagawa, A. Kawamoto and K. Hiraki, Synth. Metals **103**, 1825 (1999).
 - ²² Y. Nogami, K. Oshima, K. Hiraki and K. Kanoda, J. Phys. IV France **9**, 357 (1999).
 - ²³ M. Meneghetti, C. Pecile, K. Kanoda, K. Hiraki and K. Yakushi, Synth. Metals **120**, 1091 (2001).
 - ²⁴ T. Miyazaki, K. Terakura, Y. Morikawa and T. Yamasaki, Phys. Rev. Letters **74**, 5104 (1995).
 - ²⁵ D.S. Chow, F. Zamborszky, B. Alavy, D.J. Tantillo, A. Baur, C.A. Merlic and S. Brown, Phys. Rev. Letters **85**, 1698 (2000).
 - ²⁶ H.H.S. Javadi, R. Laversanne and A.J. Epstein, Phys. Rev. **B 37**, 4280 (1988).
 - ²⁷ F. Nad, P. Monceau, C. Carcel and J.M. Fabre, Phys. Rev. **B 62**, 1753 (2000) ; *ibid* J. Phys. Condens. Matter **12**, L435-L440 (2000).
 - ²⁸ S. Mazumdar, R.T. Clay and D.K. Campbell, Synth. Metals **120**, 679 (2001) ; R.T. Clay, S. Mazumdar and D.K. Campbell, cond-mat/0112278.
 - ²⁹ Ph. Maurel, M.-B. Lepetit and D. Poilblanc, Eur. Phys. J. **B 21**, 481 (2001).